CrossMark

ORIGINAL PAPER

Preparation, characterization and the release kinetics of mentha-8-thiol-3-one-β-cyclodextrin inclusion complex

Guangyong Zhu[1] · **Zuobing Xiao**[1] · **Guangxu Zhu**[2]

Abstract Mentha-8-thiol-3-one, with a characteristic black currant flavor, has been widely used in blending flavors and perfumes. To improve its shelf-life and stability, and control its release, mentha-8-thiol-3-one-β-cyclodextrin inclusion complex was produced. The inclusion complex was characterized by transmission electron microscopy, Fourier transform infrared spectroscopy and X-ray diffraction. Kinetics and release characteristics of mentha-8-thiol-3-one from the inclusion complex were determined by thermogravimetric analysis. The results showed that mentha-8-thiol-3-one was successfully encapsulated in β-cyclodextrin, and the loading capacity was about 13.5 %. The inclusion complex aggregates had many geometric shapes and the particle size was mostly in the range of 1–3 μm. The distributions of S, C and O can be observed element maps of mentha-8-thiol-3-one-β-CD inclusion complex. Mentha-8-thiol-3-one release from the inclusion complex mainly occurred in the first stage of pyrolysis. At 236.3 °C, the release rate of mentha-8-thiol-3-one attained the maximum value. The release reaction order was 1.5. The apparent activation energy and pre-exponential factor were 290.8 kJ/mol and 3.19×10^{24}, respectively.

Keywords Encapsulation · Release · Kinetics · Mentha-8-thiol-3-one · Inclusion complex

✉ Zuobing Xiao
  zbingxiao@sina.com

1   School of Perfume and Aroma Technology, Shanghai Institute of Technology, No. 100 Haiquan Road, Shanghai 201418, People's Republic of China

2   14846, 43 Ave., Edmonton, AB T6H 5S1, Canada

Introduction

Mentha-8-thiol-3-one, with a synonym mercaptomenthone, was found in buchu oil. As an ingredient of flavor, it has a black currant flavor. Furthermore, it has fruity, minty, sulfurous and catty, metallic, buchu-like, with a cooling, green tropical nuance, winey, slightly durnianlike, grape, blackcurrant, blackberry with a somewhat creamy mouthfeel taste characteristics at 5 ppm [1]. Mentha-8-thiol-3-one has been widely used in flavors such as green tea, oolong tea, grapefruit, tropical fruit, guava, aloe, mango, peach, tutti frutti, mint, and in alcoholic and nonalcoholic beverages, baked goods, frozen dairy, gelatins puddings and soft candy [2–6]. Mentha-8-thiol-3-one contains a sulfur atom in the molecule (Fig. 1a). These kinds of compounds containing sulfur atom usually have a powerful unpleasant and aggressive smell in the pure state; however, under suitable conditions of dilution, they may play important roles in flavor, and develop quite pleasant odors
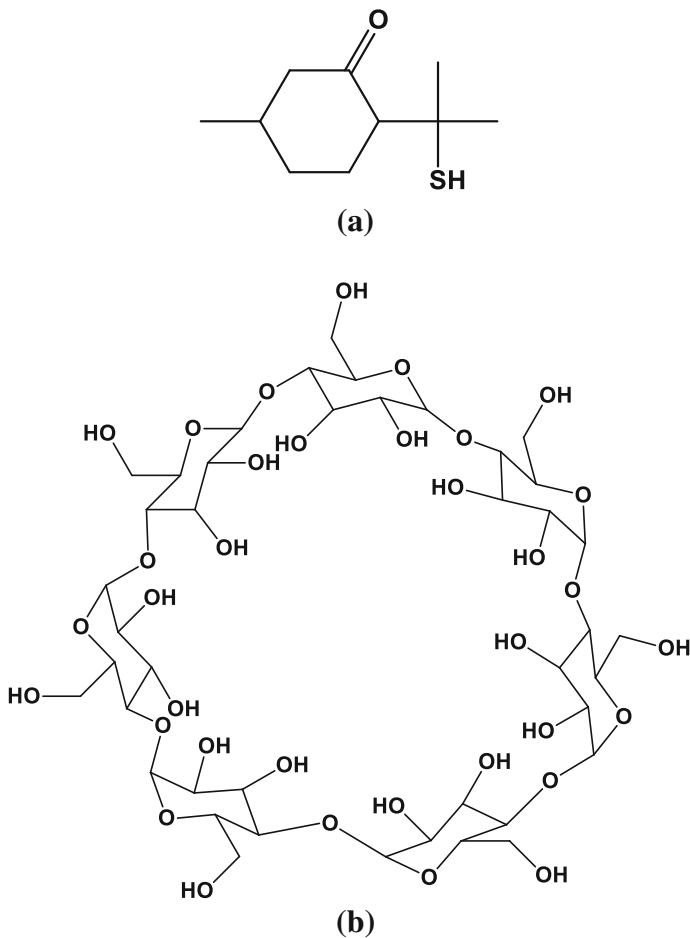
Fig. 1 The structure of menthe-8-thiol-3-one (**a**) and β-CD (**b**)

and tastes [7]. At low concentrations, mentha-8-thiol-3-one can confer a very special character to perfume, and can produce a very fresh and diffusive top note. Therefore, it is also a useful ingredient for the preparation of perfumes and perfumed products [8]. However, mentha-8-thiol-3-one has high volatility and its shelf-life is not long. Its sensory perception can be changed easily as a result of heating, oxidation, chemical interactions or volatilization. Encapsulation technology is an effective method to minimize the harm of these problems [9]. As a coating material, β-cyclodextrin (β-CD) has been widely used in microencapsulation [10–12]. β-CD has a hydrophobic inner cavity and a hydrophilic outer surface, and can encapsulate hydrophobic compounds with suitable dimensions (Fig. 1b). The inclusion complexes formed by β-CD can stabilize volatile compounds by reducing or eliminating any losses through evaporation, improve the physical and/or chemical stability of the entrapped ingredients, and avoid the destruction of certain flavors by processing or, on storage [13].

In this paper, the production and characterization of mentha-8-thiol-3-one-β-CD inclusion complex inclusion complex were investigated. The products were characterized by transmission electron microscopy (TEM), Fourier transform infrared (FTIR) spectroscopy, X-ray diffraction (XRD) and thermogravimetric (TG) analysis. The mentha-8-thiol-3-one release characteristics from the mentha-8-thiol-3-one-β-CD inclusion complex and release apparent activation energy were determined.

Materials and methods

Materials

Mentha-8-thiol-3-one ($C_{10}H_{18}OS$) was provided by the Peking University Zoteq Co. Ltd. Anhydrous ethanol and β-CD ($C_{42}H_{70}O_{35}$, white crystalline powder, pharmaceutical grade) were provided by Shanghai Sinopharm Chemical Reagent Co. Ltd. Throughout the experiments, deionized water was used. All reagents were used without further purification.

Production process of mentha-8-thiol-3-one-β-CD inclusion complex

The method of preparation of mentha-8-thiol-3-one-β-CD inclusion complex was adopted as described in the literatures [14–16]. 3 g of β-CD was dissolved in 100 g of deionized water. The temperature was kept at 35 °C on a hot plate. Then, 2 g mentha-8-thiol-3-one was slowly added to the warm β-CD solution. The mixture was continuously stirred for another 3 h and the temperature maintained at 35 °C to form mentha-8-thiol-3-one-β-CD inclusion complex. When its temperature decreased spontaneously to room temperature, the solution was refrigerated overnight at 5 °C. The cold precipitated material was recovered by vacuum filtration. The precipitate was washed by anhydrous ethanol and dried in a FD-1C-50 freeze drier for 48 h at a temperature lower than −50 °C and pressure of around 20×10^{-3} kPa. The dried mentha-8-thiol-3-one-β-CD inclusion complex sample

was collected and stored in a desiccator at room temperature. This sample was used for further TEM, FTIR, TG and XRD analysis.

Morphology and element map measurement

To investigate the morphology and the component of mentha-8-thiol-3-one-β-CD inclusion complex, TEM and element map measurement was conducted using a FEI Tecnai electron microscopy (TECNAI G2) at an acceleration voltage of 200 kv. The mentha-8-thiol-3-one-β-CD inclusion complex aqueous solution was dripped onto a 300 mesh carbon-coated copper grid. Before viewing on the transmission electron microscopy, the sample was dried under an infrared lamp.

Fourier transform infrared (FTIR) spectroscopy measurements

Mentha-8-thiol-3-one, β-CD and the mentha-8-thiol-3-one-β-CD inclusion complex were characterized by IR spectrometry. The FTIR measurements were performed with a Fourier-Transform-Spectrometer (IRAffinity-1, Shimadzu Company, Japan). The spectra have a resolution of 2 cm^{-1} and the frequency ranges from 600 to 4000 cm^{-1}.

X-ray diffraction (XRD)

XRD patterns of β-CD and the mentha-8-thiol-3-one-β-CD inclusion complex were investigated by an X-ray diffractometer (D/Max 2000X, Rigaku Corporation, Japan). The patterns were recorded in the region of 2θ from 5° to 70° with Cu Kα radiation at 40 kV and 100 mA.

Thermogravimetric analysis

The thermogravimetric experiments were investigated in a TGA-Q5000IR thermogravimetric analyzer (TA Instruments, USA) to measure and record the weight loss with temperature over the course of the pyrolysis reaction. The tested sample, approximately 5 mg, was loaded and spread uniformly on the bottom of the ceramic crucible of the thermal analyzer in the experiment. In a dynamic high purity nitrogen flow of 20 ml/min, the pyrolysis experiment was carried out at a heating rate of 10 °C/min. Nitrogen gas was used as an inert purge gas to displace air in the pyrolysis zone, thus avoiding unwanted oxidation of the sample. The heating temperature in the thermogravimetric experiments ranged from room temperature to 500 °C.

Results and discussion

Morphology and element map of mentha-8-thiol-3-one-β-CD inclusion complex

Mentha-8-thiol-3-one is hydrophobic and insoluble in water. β-Cyclodextrin has a relatively hydrophobic cavity. Therefore, in aqueous solution, β-cyclodextrin can

accommodate mentha-8-thiol-3-one to form inclusion complex. The inclusion complex of mentha-8-thiol-3-one with β-CD was observed by transmission electron microscopy and a selected micro-photograph is shown in Fig. 2. In general, large aggregates can be formed in β-CD inclusion complex aqueous suspension [17]. From Fig. 2, we can see that the aggregates can take on many geometric shapes. Most of the dried mentha-8-thiol-3-one-β-CD inclusion complexes range from 1 to 3 μm.

Energy-filtered TEM of mentha-8-thiol-3-one-β-CD inclusion complex was taken to further clarify the component and the distribution of mentha-8-thiol-3-one. Figure 3 shows the element maps of mentha-8-thiol-3-one-β-CD inclusion complex. It can be seen that the S, C and O elements are present in the sample. Figure 3a shows the overlap of all elements (C, O and S) in the composite. The distributions of S, C and O can be observed in Fig. 3b–d, respectively. The S element comes from mentha-8-thiol-3-one. It reflects the distribution of mentha-8-thiol-3-one in the inclusion complex. As shown in Fig. 3b, few particles are seen on the S map due to low amount of S in the mentha-8-thiol-3-one-β-CD inclusion complex. However, the signal of C is clear and can also be seen in the other regions of map as shown in Fig. 3c. This is due to high amount of C and the carbon-coated copper grid used in TEM measurement.

The curves of FTIR spectra of mentha-8-thiol-3-one, β-CD and its inclusion complex

Figure 4a shows the FTIR spectra of mentha-8-thiol-3-one, β-CD and the inclusion complex. In the FTIR curve of mentha-8-thiol-3-one, the asymmetrical and the
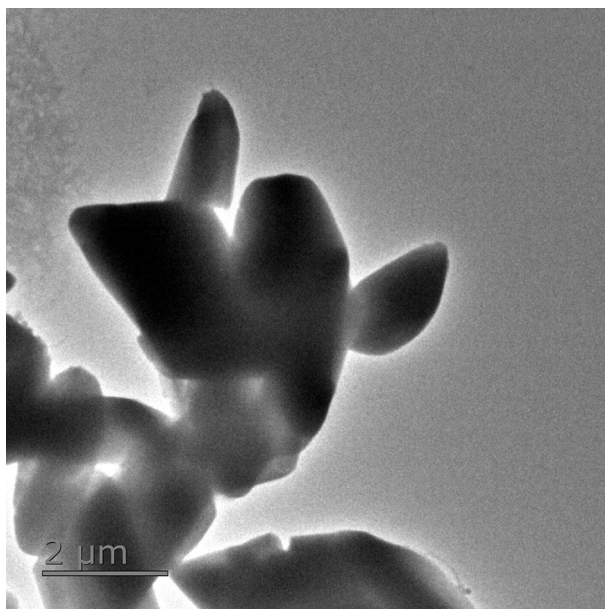
**Fig. 2** TEM photo of mentha-8-thiol-3-one-β-CD inclusion complex
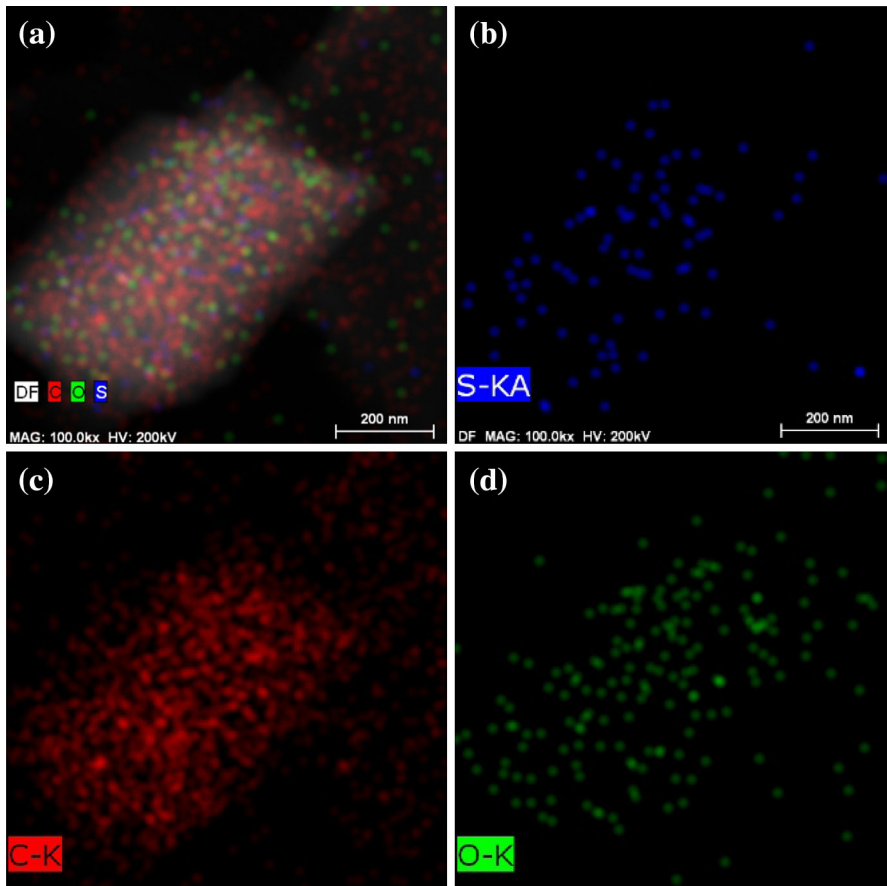
Fig. 3 Element maps of mentha-8-thiol-3-one-β-CD inclusion complex [**a** the overlap of all elements, **b** S element, **c** C elements, **d** O element]

symmetrical C–H stretching vibrations of (CH$_3$–) occur at 2955 and 2872 cm^{-1}, respectively [18]. The S–H stretching was reported in the region 2650–2550 cm^{-1} [19]. In the light of the above statement, the band at 2586 cm^{-1} is assigned to S–H stretching vibration. The stretching (C=O) vibration appears at 1709 cm^{-1}. The bands at 1454 and 1367 cm^{-1} are due to bending (C–H) vibration of (CH$_3$–) [20].

In the FTIR curve of β-CD, the stretching (O–H) vibration of hydroxyl group appears at 3337 cm^{-1}. A broad band can be observed at this region. A band at 1151 cm^{-1} and a strong band at 1030 cm^{-1} can be assigned to stretching (C–O) vibration [15].

The FTIR curve of mentha-8-thiol-3-one-β-CD inclusion complex and that of blank β-CD are similar. This indicates that the frame of β-CD in the complex is not changed. Encapsulation of mentha-8-thiol-3-one does not cause significant changes of spectra of β-CD. Compared with the curve of β-CD, the stretching (O–H) vibration of hydroxyl group in the curve of inclusion complex shifted from 3337 to
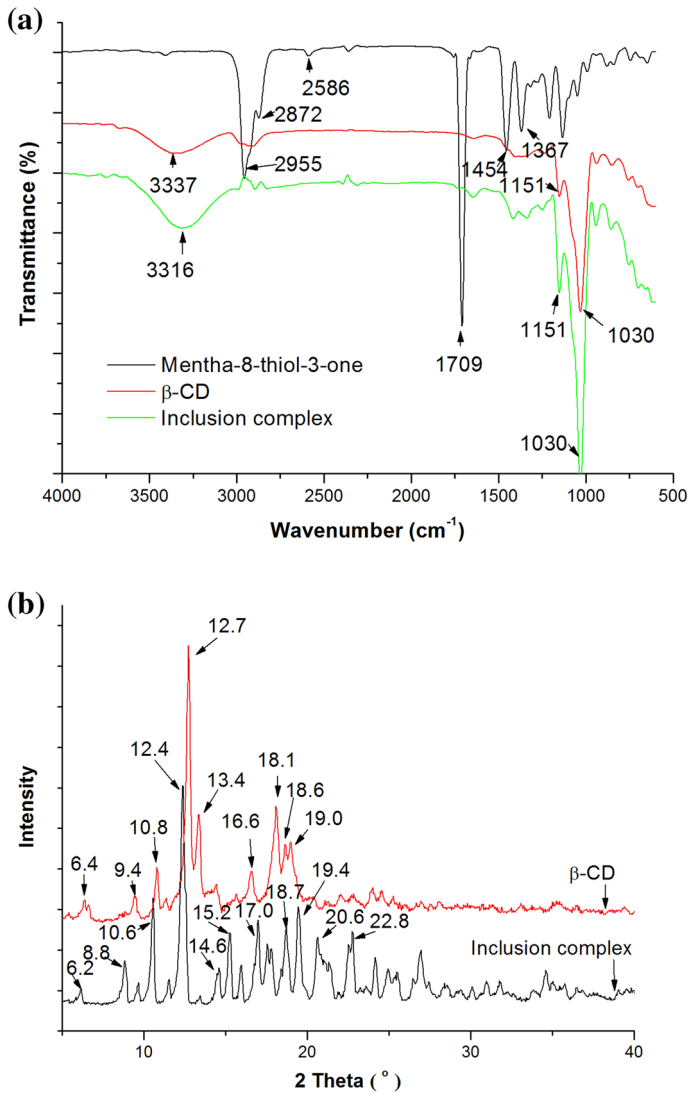
Fig. 4 FTIR spectra (**a**) and XRD patterns (**b**) of β-CD and mentha-8-thiol-3-one-β-CD inclusion complex

3316 cm^{-1}. The strong peak at 1709 cm^{-1} in the curve of mentha-8-thiol-3-one has a noticeable change and this peak disappears in the curve of the inclusion complex. Furthermore, the bands of mentha-8-thiol-3-one at 2955, 2872, 1454 and 1367 cm^{-1} disappear or shift to other wave numbers in the curve of the inclusion complex. From these changes, it can be deduced that mentha-8-thiol-3-one was encapsulated into the cavity of β-CD.

XRD results of β-CD and inclusion complex

XRD is a useful method for the detection of CD inclusion complex. In order to see if in fact mentha-8-thiol-3-one was encapsulated in β-CD and crystalline or amorphous, XRD was also used to characterize β-CD and the inclusion complex. The curve of XRD has sharp peaks for crystalline substance and, however, no peaks for amorphous materials. Menthe-8-thiol-3-one is a liquid and XRD is not suitable for determination of liquids. The results of XRD are shown in Fig. 4b. As shown in Fig. 4b, the peaks at 12.7°, 10.8° and 6.4° in the XRD pattern of β-CD shift to 12.4°, 10.6° and 6.2°, respectively, in the XRD pattern of the inclusion complex. In contrast, the peaks of 18.1°, 18.6° and 19.0° for β-CD shifted to lower 2θ angle of 17.0°, 17.6° and 17.8° for the inclusion complex. A similar result was also reported for the peak shift [21]. Furthermore, the peaks at 9.4°, 13.4° and 16.6° of β-CD disappear in the XRD pattern of inclusion complex. Some new peaks at 8.8°, 19.4°, 20.6° and 22.8° appear in the XRD pattern of mentha-8-thiol-3-one-β-CD inclusion complex. From these changes and the results of FTIR, it can be inferred that mentha-8-thiol-3-one was encapsulated in the cavity of β-CD.

Thermogravimetric characteristics

The TG and DTG curves obtained during the pyrolysis of blank β-CD and mentha-8-thiol-3-one-β-CD inclusion complex under inert atmosphere at a heating rate of 10 °C/min are shown in Fig. 5a. During the heating process of β-CD and mentha-8-thiol-3-one-β-CD-β-CD inclusion complex, three stages can be observed during thermal degradation. In the TG curve of β-CD, the first stage refers to the temperature range from room temperature to 282 °C and the weight loss in this stage is 4.4 %. This could be due to the loss of water and light volatile compounds. In the TG curve of mentha-8-thiol-3-one-β-CD-β-CD inclusion complex from room temperature to 282 °C, the weight loss is 17.9 %. The weight loss of mentha-8-thiol-3-one-β-CD-β-CD inclusion complex is much larger than that of β-CD. This is mainly due to mentha-8-thiol-3-one encapsulated in the cavity of β-CD. The difference in the two values of weight loss is 13.5 %. From the difference, mentha-8-thiol-3-one loading capacity can be estimated as about 13.5 %. In DTG curve of mentha-8-thiol-3-one-β-CD inclusion complex, a small peak appears at 236.3 °C. It can be attributed to the release of mentha-8-thiol-3-one-β-CD encapsulated in the cavities of β-CD. At this temperature, the rate of weight loss attained the maximum value. In the TG curve of β-CD, the second stage refers to the temperature range from 282 to 372.7 °C. The second stage was characterized by a major weight loss, which corresponded to the main pyrolysis process of β-CD. Most of β-CD was decomposed in this stage. In the second stage, two strong peaks can be observed in the DTG curves of β-CD and mentha-8-thiol-3-one inclusion complex, respectively. The two strong peaks were due to the decomposition of β-CD. Compared with the DTG curve of β-CD, the strong peak in the DTG curve of mentha-8-thiol-3-one inclusion complex shifted to a lower temperature and its intensity decreased. These changes may be due to mentha-8-thiol-3-one encapsulated in the cavity of β-CD. In the TG curve of β-CD, the third stage refers to the temperature range from 372.7 °C
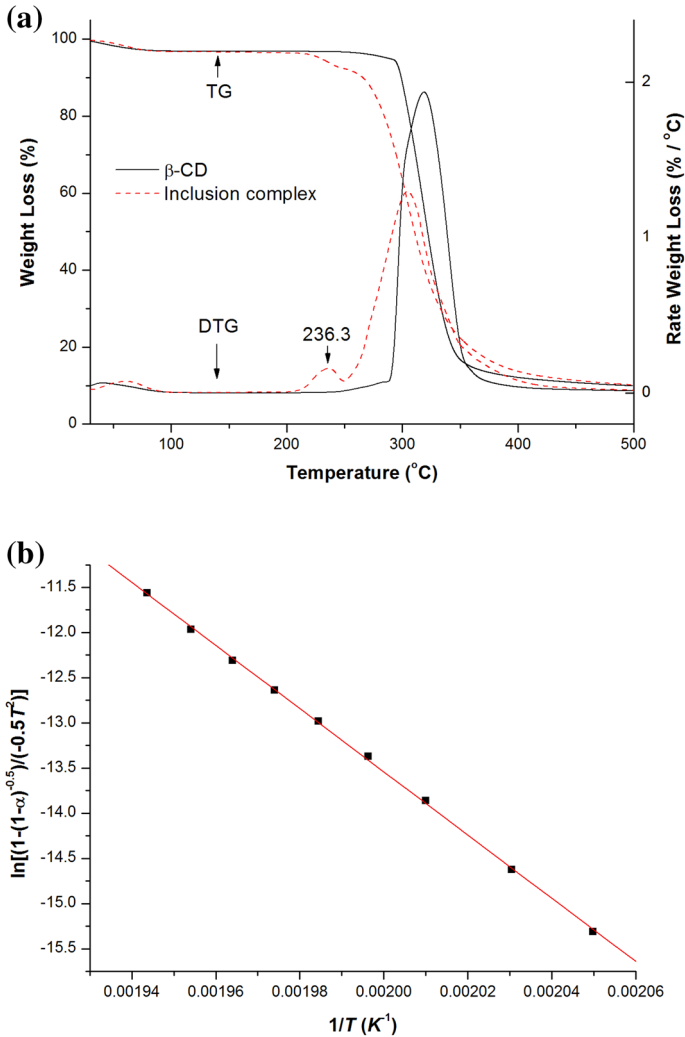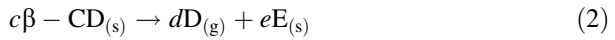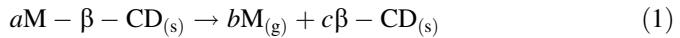
Fig. 5 Weight loss and rate of weight loss curves of mentha-8-thiol-3-one-β-CD inclusion complex and blank β-CD at a heating rate of 10 °C/min (**a**), and plot of $\ln[(1-(1-\alpha)^{-0.5}/(-0.5T^2)]$ vs. $1/T$ (**b**)

to the final temperature (500 °C). In the third stage, the solid residuals continuously decomposed at a very slow rate. Slight weight losses can be observed in TG curves of both β-CD and mentha-8-thiol-3-one-β-CD inclusion complex.

Release kinetic parameters of mentha-8-thiol-3-one-β-CD from inclusion complex

The thermogravimetric data can be used to evaluate kinetic parameters of solid-state reactions. This method was reported in a number of literatures [14, 16].

Equations (1) and (2) can be simply used to express the pyrolysis reaction of the mentha-8-thiol-3-one-β-CD inclusion complex.

$$aM - \beta - CD_{(s)} \rightarrow bM_{(g)} + c\beta - CD_{(s)} \quad\quad (1)$$

$$c\beta - CD_{(s)} \rightarrow dD_{(g)} + eE_{(s)} \quad\quad (2)$$

where M-β-CD is the mentha-8-thiol-3-one-β-CD inclusion complex in the solid state, M is the mentha-8-thiol-3-one in gas state, D is a volatile product, and E is the other product in the condensed state.

During the pyrolysis process of mentha-8-thiol-3-one-β-CD inclusion complex, firstly, mentha-8-thiol-3-one releases from the inclusion complex. Secondly, the resulting β-CD decomposes to further products when the temperature is above 282 °C.

Equation (3) can be used to express the disappearance rate of Menthol-HP-β-CD in the reaction as shown in Eq. (1).

$$\frac{d\alpha}{dt} = k(1 - \alpha)^n \quad\quad (3)$$

where n is the order of reaction, α is the fraction of mentha-8-thiol-3-one-β-CD decomposed at time t, and k is the rate constant.

The integrated forms of Eq. (3) can be expressed as Eqs. (4) and (5) according to Coats and Redfern method [22].

$$\ln\left[\frac{1 - (1 - \alpha)^{1-n}}{T^2(1 - n)}\right] = \ln\left(\frac{AR}{\gamma E}\right) - \frac{E}{RT} \quad (\text{for } n \neq 1) \quad\quad (4)$$

$$\ln\left[\frac{-\ln(1 - \alpha)}{T^2}\right] = \ln\left(\frac{AR}{\gamma E}\right) - \frac{E}{RT} \quad (\text{for } n = 1) \quad\quad (5)$$

where E is the apparent activation energy, A is the pre-exponential factor, γ is the heating rate, R is the gas constant, and T is the absolute temperature.

For a correct value of n, a plot of either $\ln[-\ln(1-\alpha)/T^2]$ against $1/T$ or, where $n \neq 1$, $\ln[(1-(1-\alpha)^{1-n})/T^2/(1-n)]$ against $1/T$ should result in a straight line of slope $-E/R$. From the intercept and slope of the line, the pre-exponential factor and the apparent activation energy of the dynamic degradation at various conversions can be estimated, respectively.

The small peak, which appears at 236.3 °C in the rate of weight loss curve of the mentha-8-thiol-3-one-β-CD inclusion complex in the first stage as shown in Fig. 5a, is due to the release of mentha-8-thiol-3-one encapsulated in β-CD. This peak was used to investigate mentha-8-thiol-3-one-β-CD release kinetic parameters. Different reaction orders were selected for mentha-8-thiol-3-one-β-CD inclusion complex to fit straight line in the experiments. Table 1 shows all the squared values of linear correlation coefficients (R^2) calculated from Eqs. (4) to (5) by fitting the experiment data.

The closer are the squared values of linear correlation coefficients to 1, the better the linear relationship between $\ln[-\ln(1-\alpha)/T^2]$ and $1/T$ or between

Table 1 The squared values of linear correlation coefficents (R^2) calculated by fitting the experiment data

Peak temperature	$n = 0$	$n = 0.5$	$n = 1$	$n = 1.5$	$n = 2$	$n = 2.5$	$n = 3$
236.3 °C	0.9731	0.9870	0.9959	0.9995	0.9981	0.9926	0.9844

Table 2 The values of apparent activation energy and reaction order obtained from the intercept and the slope of the fitting line

n	T (°C)	a (%)	E (kJ/mol)	a
1.5	214.7–241.3	5–80	290.8 ± 2.4	3.19×10^{24}

$\ln[(1-(1-\alpha)^{1-n})/T^2/(1-n)]$ and $1/T$ should be. The squared value of linear correlation coefficient is relatively closer to 1 when reaction order, n, is 1.5. Therefore, 1.5 was used as the pyrolysis reaction order for peak at 236.3 °C. Figure 5b shows the plots of $\ln[(1-(1-\alpha)^{-0.5})/(-0.5T^2)]$ against $1/T$. There is a good linear relationship between $\ln[(1-(1-\alpha)^{-0.5}/(-0.5T^2)]$ and $1/T$ when the value of reaction order is 1.5 for peak at 236.3 °C as shown in Fig. 5b. The value of R^2 is greater than 0.999. The plot has a high linear correlation coefficient.

From the intercept of the line, the pre-exponential factor can be calculated. The apparent activation energy can be estimated from the slope of the line. The value of pre-exponential factor and apparent activation energy obtained from the intercept and the slope of the line by fitting the experiment data according to Eq. (4) are given in Table 2. The pre-exponential factor value (3.19×10^{24}) is higher compared with the values of sweet orange flavor-β-CD inclusion complex (4.32×10^{12}) [14] and lavender-HP-β-CD inclusion complex (1.0×10^8) [16].

In chemistry, activation energy is a term to describe the minimum energy which must be available to a chemical system with potential reactants to result in a chemical reaction. Low activation energy means a fast reaction and high activation energy means a slow reaction according to the Arrhenius equation. Activation energy may also be defined as the minimum energy required starting a chemical reaction and can be thought as the energy barrier separating mentha-8-thiol-3-one from mentha-8-thiol-3-one-β-CD inclusion complex. It can reflect the combination of mentha-8-thiol-3-one and β-CD. Small activation energy indicates that mentha-8-thiol-3-one easily releases from the inclusion complex and the mentha-8-thiol-3-one-β-CD inclusion complex is instable, while high activation energy implies that mentha-8-thiol-3-one is bound to β-CD firmly and the mentha-8-thiol-3-one-β-CD inclusion complex is relatively stable. The apparent activation energy is positive. It means that energy is required to disassemble a whole mentha-8-thiol-3-one-β-CD into separate parts. The value of apparent activation energy (290.8 kJ/mol) is higher compared with the values of sweet orange flavor-β-CD inclusion complex (104.5 kJ/mol) [14] and lavender-HP-β-CD inclusion complex (86.4 kJ/mol) [16]. From the apparent activation energy value obtained as shown in Table 2, we can infer that the mentha-8-thiol-3-one-β-CD inclusion complex is relatively stable.

Conclusions

Mentha-8-thiol-3-one-β-CD inclusion complex was successfully produced and characterized. The morphology of mentha-8-thiol-3-one inclusion complex takes on many geometric shapes. The distribution of mentha-8-thiol-3-one was reflected by element map. The results of FTIR, XRD and TG confirmed that mentha-8-thiol-3-one entered the cavity of β-CD. The mentha-8-thiol-3-one loading capacity was determined by TG analysis, and the value is about 13.5 %. During the thermal degradation of mentha-8-thiol-3-one-β-CD inclusion complex, Mentha-8-thiol-3-one release from the inclusion complex mainly occurred in the temperature range from room temperature to 282 °C, especially at 236.3 °C. At this temperature, the rate of mentha-8-thiol-3-one release attained the maximum value. The release reaction order, apparent activation energy and pre-exponential factor were determined and the values were 1.5, 290.8 kJ/mol and 3.19×10^{24}, respectively.

References

1. Burdock GA (2010) Fenaroli's handbook of flavor ingredients. CRC Press, Boca Raton
2. Ai P (2006) The study on aloe flavour. J Shanghai Inst Technol 3:284–286 **(in Chinese)**
3. Emura M, Masumura S, Maruyama K, Yamamoto T (2013) Flavor and fragrance compositions. US Patent: 8575086 B2
4. X-l Fang (2006) The Manufacture of Guava Flavor. Mod Food Sci Technol 22:177–178 **(in Chinese)**
5. M-b Zhang (2013) Aromatic theme mango flavor. China Food Addit 3:198–204 **(in Chinese)**
6. Zhu G, Xiao Z (2015) Study on creation of an indocalamus leaf flavor. Food Sci Technol Campinas 35(4):647–651
7. Zhu G, Xiao Z, Zhou R, Lei D (2015) Preparation and simulation of a taro flavor. Chin J Chem Eng 23:1733–1735
8. Sundt E, Ohloff G (1977) Menthone-8-thiol, carvomenthone-8-thiol and process for preparing same. US Patent: 4034044
9. Zhu G, Xiao Z, Zhou R, Yi F (2012) Fragrance and flavor microencapsulation technology. Adv Mater Res 535–537:440–445
10. Aytac Z, Kusku SI, Durgun E, Uyar T (2016) Quercetin/β-cyclodextrin inclusion complex embedded nanofibres: slow release and high solubility. Food Chem 197:864–871
11. Bonetti P, Moraes FFd, Zanin GM, Bergamasco RdC (2016) Thermal behavior study and decomposition kinetics of linalool/β-cyclodextrin inclusion complex. Polym Bull 73:279–291
12. Olga G, Styliani C, Ioannis RG (2015) Coencapsulation of ferulic and gallic acid in hp-b-cyclodextrin. Food Chem 185:33–40
13. Marques HMC (2010) A review on cyclodextrin encapsulation of essential oils and volatiles. Flavour Frag J 25:313–326
14. Zhu G, Xiao Z, Zhou R, Zhu Y (2014) Study of production and pyrolysis characteristics of sweet orange flavor-β-cyclodextrin inclusion complex. Carbohyd Polym 105:75–80
15. Zhu G, Feng N, Xiao Z, Zhou R, Niu Y (2015) Production and pyrolysis characteristics of citral–monochlorotriazinyl-β-cyclodextrin inclusion complex. J Therm Anal Calori 120:1811–1817
16. Zhu G, Xiao Z, Zhou R, Feng N (2015) Production of a transparent lavender flavour nanocapsule aqueous solution and pyrolysis characteristics of flavour nanocapsule. J Food Sci Tech 52:4607–4612
17. He Y, Fu P, Shen X (2008) Cyclodextrin-based aggregates and characterization by microscopy. Micron 29:495–516

18. H-y Si, G-f Sun, Z-k Zhu (2010) Preparation of menthone by chromic acid oxidation. Shandong Chem Ind 39:15–17 **(in Chinese)**
19. Prabavathi N, Nayaki NS (2014) The spectroscopic (FT-IR, FT-Raman and NMR), first order hyperpolarizability and HOMO–LUMO analysis of 2-mercapto-4(3H)-quinazolinone. Spectrochim Acta A 129:572–583
20. Fan K (2011) An introduction to spectroscopy. Higher Education Press, Beijing **(in Chinese)**
21. Yang Z, Xiao Z, Ji H (2015) Solid inclusion complex of terpinen-4-ol/β-cyclodextrin: kinetic release, mechanism and its antibacterial activity. Flavour Frag J 30:179–187
22. Coats AW, Redfern JP (1964) Kinetic parameters from thermogravimetric data. Nature 201:68–69